JJBS

Jordan Journal of Biological Sciences

Comparative Studies on Antibacterial Activities of Chitosan, Silver Nanoparticles and Maggot Based chitosan-silver Nanocomposites Against Fish Pathogens.

Joseph A. Olugbojo[1,*], Adeolu A. Akinyemi[2], Samuel O. Obasa[2], and Enock O. Dare[3]

[1]Department of Biological Sciences, Bells University of Technology, Ota, Ogun State, Nigeria; [2]Department of Aquaculture and Fisheries Management, Federal University of Agriculture, Abeokuta, Ogun State, Nigeria; [3]Department of Chemistry, Federal University of Agriculture, Abeokuta, Ogun State, Nigeria

Abstract

The current study explored the *ex- situ* bio-fabrication of maggot-based chitosan-silver nanocomposites (CS-AgNCs), silver nanoparticles (AgNPs) and chitosan (CS). It was conducted in view of an increasing demand to replace antibiotics with nanomaterials due to their eco-friendliness, non-hazardous and biocompatibility. AgNPs were prepared using *Cassia fistula* leaf extract as bio-reductant, CS was prepared from maggot chitin, while *ex-situ* bio-fabrication technique was used to synthesize CS-AgNCs. The integrity of the formed nanoparticles and polymer composites were established through ultra violet-visible (UV-Vis.) spectrophotometry, Fourier transform infrared (FTIR) spectroscopy, X-ray diffraction (XRD), scanning electron microscopy (SEM), and energy dispersive x-ray (EDX) analysis. To evaluate and compare their antibacterial potency, *Aeromonas schubertii, Aeromonas hydrophila, Vibrio parahaemolyticus, Klebsiella aerogene* and *Proteus mirabilis* strains were selected as test organisms. Antibacterial activity tests were carried out using agar well diffusion technique. Data collected were subjected to analysis of variance (ANOVA). The result depicted hexagonal and cuboidal AgNPs and CS respectively, while CS-AgNCs were observed as chitosan matrix embedded with AgNPs. The average particle size of AgNPs, CS and CS-AgNCs were 24.94 nm, 30.95 nm and 65.03 as observed on SEM. The XRD analysis showed that they were all crystalline in nature. *In-vitro* antibacterial activities revealed a marked difference ($P<.0.05$) in the inhibition zones after tested the nanoparticles and the polymer composites on each of the bacteria except CS-AgNC and CS, whose difference are not significant ($P>.0.05$) when tested on *V. parahaemolyticus* (16.00 ± 1.15 and 15.50 ± 1.73) mm and *P. mirabilis* (19.00 ± 2.31 and 19.00 ± 1.15) mm. This outcome clarified that the polymer composites were the most effective against the test bacteria whose zone of inhibition was highest, ranging from 15.00 ± 2.31 mm to 22.50 ± 0.58 mm, followed by chitosan; 12.50 ± 0.58 mm to 19.00 ± 1.15 mm and least in AgNPs; 8.00 ± 1.15 mm to 13.00 ± 1.15 mm. Consequently, maggot-based chitin from which chitosan was produced is rarely used to produce chitosan, thus making CS-AgNP a novel nanocomposite, which can be used for pond water treatment and fish diseases associated with the test pathogens.

Key words: Bio-fabrication, Maggot-based chitin, Nano-antibacterial, Polymer composites, Scanning electron microscopy, Silver nanoparticles, X-ray Diffraction.

1. Introduction:

The problem of pathogenic bacteria has limited effective fish production and availability in global aquaculture industry. Among fish diseases, those caused by bacteria spread widely than those caused by other pathogens, and have brought much distress due to serious economic losses through high mortality (Olugbojo and Ayoola, 2015). Increase in resistance of various bacteria to several antibiotics has also limited a gainful treatment and thus emphasized the need to develop a new antimicrobial (Quesada *et al*., 2013). In addition, available literature has shown that there are limited reports on the use of nanoparticles for prophylactic and therapeutic treatment in aquaculture, especially on evaluation of antibacterial activity of silver nanoparticles using *Cassia fistula* as bioreductant, Chitosan, and Maggot–based Chitosan silver nanocomposites on pathogenic bacteria isolates such as: A. *schubertii, A. hydrophila, V. parahaemolyticus, K. aerogene* and *P. mirabilis* from *Clarias gariepinus (*African mud catfish) in Nigeria.

From the literature search, there has not been previous work on antibacterial sensitivity of *A. schubertii* using Chitosan, silver nanoparticles, and Chitosan silver nanocomposites as antibacterial agents, apart from some antibiotics which have been used to control *A. schubertii* infections in some fishes. *A. schubertii* is a rare *Aeromonas sp* pathogen in fish, and there is lesser report on its incidence or outbreak in fish farms, the prevalent

* Corresponding author. e-mail: josephgbojo2012@gmail.com.

ones being *A. hydrophila, A. veronii, and A. Caviae.* However, *A. schubertii* was first reported in brackish water wild tilapia (*Oreochromis niloticus*) in China by Zhuling *et al.* (2019). It was noted that the natural infection route was through damage on fish skin and digestive tract. Moreover, antibiotic sensitivity test carried out showed that *A. schubertii* was susceptible to Norflorxacin and Rifampicin but resistant to several other antibiotics. Chen *et al* (2012) also isolated and characterized *A. schubertii* from a diseased snakehead fish (*channel maculate* - Lacepede) suffering high mortality. *In-vitro* antibiotic susceptibility test revealed that it was susceptible to cefoxitin, cefoperazone, and chloramphenicol. Also, Thai *et al* (2023) discovered a prevalence and antibiotic resistant *A. schubertii* causing internal white spot diseases on another snake head fish (*C. striata*) in the Mekong delta, Vietma. The antibiotic susceptibility test also revealed that all the identified isolates of *A. schubertii* were phenotypically multi drug resistant. The multiple antibiotic resistance index ranged from 0.33 to 0.92, being resistant against 11 out of 12 tested antibiotics, showing that *A. schubertiii* was responsible for white spot diseases in snake head fish. All report so far has been that *A. schubertii* was highly resistant to varieties of antibiotic drug while being sensitive to some.

For a long time, *K. aerogene* and *P. mirabilis* have been considered as opportunistic pathogens; however, Zhai *et al* (2023) in his research on the outbreak of *A. veronii* and *P. mirabilis* in yellow catfish and channel catfish discovered that *P. mirabilis*, has a high potential with grave possibility of becoming a serious threat to fish. He noted that yellow catfish were more responsive to *A. veronii* than *P. mirabilis*, while *P. mirabilis* weakens and exposes fish to infections with little resistance. The number of *A. veronii* in the *P. mirabilis* immersion challenged group increased and was 15% higher than that in the control group. This is in agreement with *P. mirabilis* making their hosts more prone to disease through the differentiation of swarmer cell with the expression of virulence factors (Zhai *et al.*, 2023). *A. veronii* causes protrusion of the abdomen and ovarian damage while *P. mirabilis* also causes distension of the abdomen and skin redness. However, *P. mirabilis* might render the host responsive to *A. veronii* attack, even though the underlying mechanism is yet to be clarified (Zhai *et al.*, 2023).

A related research conducted by Adeyemo *et al.*, (2023) validated the fact that obligatory fish pathogens share the same environment with other resident and opportunistic pathogens with the possibility of sharing and transferring genetic materials, thereby affirming the high possibility of such bacterial assuming the same status with obligatory bacteria fish pathogen. This report is in consonant with Adeshina *et al.* (2016) who reported same on pathogenic *Klebsiella* species in cultured African Catfish.

This study focuses on synthesis, characterization and *in-vitro* antibacterial activity of Chitosan, silver nanoparticles, and Chitosan silver nanocomposites against *A. schubertii, A. hydrophila, V. parahaemolyticus, K. aerogene* and *P. mirabilis* isolates from *C. gariepinus*.

Nanotechnology can be defined as the synthesis, characterization, and utilization of nano-sized (1-100nm) materials for the development of science (Nikalje, 2015). It deals with the materials, whose structures exhibit novel and improved physical, chemical, and biological properties, and can find wide applications both in human and veterinary medicine (Fajardo, 2022 and Abass *et al.*, 2022).

Over the centuries, the antimicrobial activities of silver based compounds against different species of micro-organisms has been well-known. The heat and chemical resistance of Silver nanoparticles (AgNPs) is responsible for its wide acceptance and utilization as antibacterial agents. Properties such as size, shape, and increasing surface oxidation which leads to the release of silver ion (Ag+) have earned it unreserved accreditation (Ghotakar *et al*, 2019). AgNP can rapidly oxidize and release silver ion because of its large surface area to volume ratio. Although the exact mode of its antibiotic activity is yet to be fully understood, it has been reported in several literatures that because of the ultra-small size of AgNP, it easily penetrates through the cell walls of pathogens, and causes cell disruptions (Aktar *et al.,* 2017). It was also reported that the generation of reactive oxygen species and free radicals causes cell membrane damage and death when silver nanoparticle is introduced especially at a nano-scaled size (Dayem et al, 2017). Since the effectiveness of any antimicrobial depends largely on the surface area to volume ratio, likewise the antimicrobial activity of any NPs also depends on how small the particle size is. When the particle size become smaller, the surface area to volume ratio also increases.

The use of Nanoparticles and their composites in treating bacteria fish diseases is rarely investigated. Among the few works that have been carried out on antibacterial effect of silver nanoparticles is the study conducted by Islam *et al.* (2021). He worked on green synthesis of AgNP and their antagonistic effect on fish larvae pathogenic bacteria using leave extract of mangrove plants (*Avicennia marina*) as reducing and stabilizing agent. The result showed the formation of nano-sized AgNP which ranges from 15-25nm. A well identified *Vibrio spp* (from fish sample) through cultural, morphological and biochemical characterization was used as test organisms. The result of antibacterial sensitivity test on various *species* of *Vibrio* showed zone of inhibition which varies between 13.00-12.00 mm, indicating efficient impact on these pathogens. Moreover, Silver (Ag) nanoparticles have high therapeutic potential and exhibit good antimicrobial activity above several other nanoparticles. It also exhibits high potency even at a very low concentration (Govindan *et al.,* 2012). In this study, *C. fistula* leaf extract was used to synthesize silver nanoparticles due to its rare use in the syntheses of nanoparticles, despite its excellent constituent phytochemicals.

Chitin is a natural polymer derived from various living organisms, while chitosan is a product of chitin through the process of deacetylation. Apart from cellulose, chitin abounds among organisms such as fungi, microorganisms, and animals whose exoskeleton are made of chitin. It can find application as antibacterial, antitumor, and immune enhancement agent (Kaur *et al*, 2013). Chitosan also possesses properties such as biodegradability, biocompatibility, non-toxicity, renewability, and bioavailability. It is mostly preferred to synthetic polymers due to its low price and high presence in living organisms. Chitosan has already gained much application in various

fields which include Biotechnology, Food Technology, Agriculture and Veterinary medicine (Younes and Rinaudo, 2015).

The utilization of polymer composites such as chitosan-silver nanocomposites in the development of novel antibacterial has attracted much attention in recent years due to their eco-friendliness and biocompatibility. They can easily be broken down by enzymes in animal body, and the degradation products are not toxic. The synergistic incorporation of metal nanoparticles in the polymeric matrix to produce polymer composites has significantly improved the potency of chitosan and its biological action against microorganism (Dayem et al, 2017). In addition, the appealing properties of chitosan-silver nanocomposites such as biocompatibility and biodegradability made it very useful in several biomedical applications including non-inflammatory reaction after application in the host's body (Nowack *et al.*, 2011).

CS–AgNC is a rare nanocomposite that has been used as antibacterial agent especially maggot based type. Chitosan present in the nanocomposite help to prolong the activity of silver on the bacterial cell while protecting the host cells from silver toxicity which is a major advantage of a silver doped chitosan nanocomposites. In this work, Silver nanoparticles were first synthesized using *C. fistula* leaf extract as bio-reductant, chitosan was also synthesized through a simple chemical method of extraction and deacetylation of cultured maggot chitin, while CS-AgNCs were synthesized through synergistic combination at ratio one to four (1:4) of Silver and Chitosan, respectively through *ex-situ* bio-fabrication techniques.

The primary aim of this research is to evaluate and compare the antibacterial activity of Chitosan, AgNPs and Chitosan – Silver nanocomposites (*in vitro*) and make recommendation to the fish farmers, researchers and fish extension workers, based on the most potent one among the three as against the usual toxic antibiotics. It also seeks to contribute significantly to sustainable development goals 1 and 2 (poverty alleviation and food security).

2. Materials and Methods

2.1. Construction of maggot production Unit (Maggotry)

The Maggotry was made of wooden culture unit according to Hezron *et al.,* (2019) with some modifications. Figure 1 shows the longitudinal section while Fig 2 shows the 3 dimensional view of the culture unit. It consists of a large chamber (1200 x 840 x 580 mm), with two lids at the top, an outermost wooden lid of 10 mm thick, and an inner lid of about 10 mm wire mesh net. The inner net lid was designed to allow house flies to enter and lay their eggs on the exposed substrate while keeping away reptiles and rodents from gaining entry. The outermost wooden lid serves as the main door. It is not supposed to be closed completely (one-quarter closed) in order to allow fresh air into the chamber. It is also used to prevent rain, and direct sunlight from reaching into the chamber. The height of the maggotry above the ground is 600 mm.
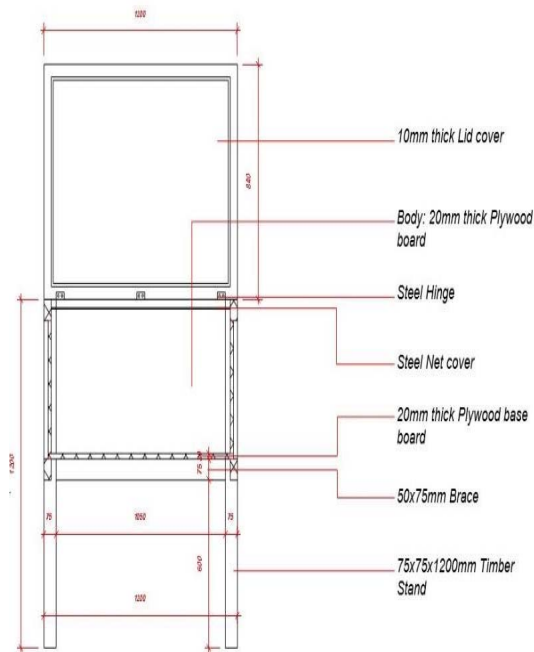

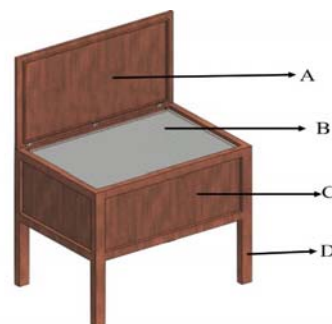**Figure 1.** A longitudinal section of Maggot culture unit

Figure: 2. 3D view of maggot culture unit.

Legend: A- Outer wooded lid. B - Inner net lid. C - Main compartment. D - Stand/Wooden leg

2.2. Culturing of housefly Maggot (Musca domestica)

The maggot of *Musca domestica* was cultured at Bells University Staff estate, Ota, Ogun State. Poultry waste was collected from Onibuku poultry farm and spread in a specially developed maggot culture unit (Figures 1 and 2). Fresh cattle blood and offal were also collected from Arobieye abattoir, Idi-Iroko road, Ota, which serve as attractants to house fly. These were added together and mixed properly to constitute substrate. The maggotry was left open for about 8-10 hrs to allow adult house fly (*M. domestica)* to converge and lay eggs, as the odour from the substrate continue to attract them. After the exposure period, a perforated black polythene sheet was used to cover the substrate so as to provide darkness in order to aid incubation and also allow water to penetrate into the substrate to prevent desiccation. The substrate was kept moisty daily to make it habitable for the prospective larvae. Larvae were harvested on the last day of the larval stage (7th day after oviposition) before they turn to pupa. They were washed, blanched with hot water, and preserved for further use (Akpodiete *et al.*, 1997; Hezron *et al.,* 2019.

2.2.1. Extraction of Chitin from maggot of Musca
   Domestica and Preparation of Chitosan

Chitin and chitosan were prepared from the maggot (larva stage) of *M. domestica* according to the method described by Kim *et al,* 2016, and Cristiano *et al*, 2019, with modifications as shown in the flow chart (Figure 3). The larval was washed to remove foreign materials and residual muscle particles using warm water. They were then dried at 50^0C in hot air oven overnight. After drying, they were grinded to 1mm particle size using Philip HR-2815 grinder. 50g of dried maggots were weighed into 250 ml conical flask and decalcified for 3 hours in 150 ml of 2M HCL solution at room temperature. It was then rinsed. The sample was soaked again in 200 ml of 1.25M NAOH at 95^0C for 3hours to remove the protein (deproteinization). It was rinsed again thoroughly with water to neutral pH and then dried for 24 hours at 70^0C in hot air oven. This process is known as chitin extraction.

Chitosan was produced from chitin through a process called deacetylation, according to the method described by Kim *et al* (2016).

2.3. Deacetylation of Chitin

Chitin extracted from maggot were boiled in 100ml of 50% NAOH (w/v) solution at 95^0C for 3 hours. The chitosan produced from chitin was washed to a neutral pH with tap water and then dried for 24hrs at 70^0C in hot air oven. It was then grinded into powder and kept in a dried place for further use.
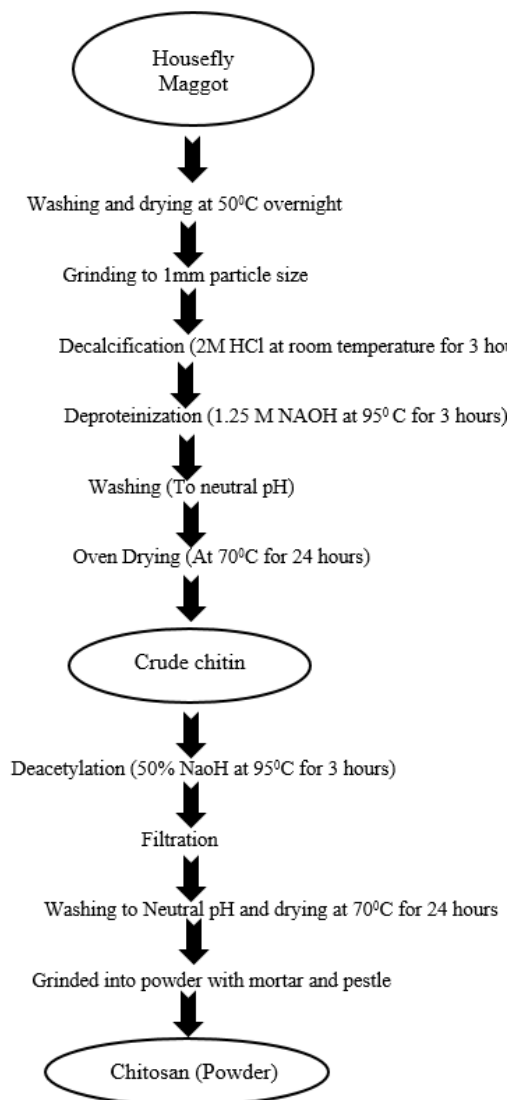

Figure 3. Flow chart of chitin and chitosan preparation

2.4 Preparation of Cassia fistula (Golden shower) leaves
   extract

Leaves of *Cassia fistula* was obtained from Covenant University, Ota Ogun state, and was authenticated in the Department of Biological Sciences Bells University of Technology, Ota by a botanist. 20g of the leaves was washed with distilled water to remove the dust particles and then air dried for about two weeks. The dried *C. fistula* leaves were cut into small pieces and boiled with 100 ml of distilled water at 70^0C for 1 hour. After boiling, the extract was cooled and separated by filtration to remove impurities, while the clear solution was used for the reduction of silver nitrate ($AgNO_3$) to silver nanoparticles (Irshad *et al.*, 2014)

2.5 Synthesis of silver nanoparticles

Silver nitrate was purchased from Sigma chemical company, U.K. (Product No. R4036/37/38). C. *fistula* (leaves) aqueous extract and 1mM $AgNO_3$ were mixed in the ratio 1:10 and heated on a hot plate with magnetic stirrer at 60^0C for 30 min until colour change (reddish

brown) was observed. The colour change indicate the formation of silver nanoparticles. The simple reaction equation and electron transfer equation leading to the formation of pure silver nanoparticles after donated the valence electron, are shown in equation 1 and 2 below.

Simple equation of reaction

$$AgNO_3 + Plant\ extract\ (C.\ fistula) \rightarrow AgNPs \qquad (1)$$

Electron transfer equation (redox reaction)

$$Ag^+ + e^- \rightarrow Ag^0 \qquad (2)$$

2.4. Preparation of Chitosan-silver nanocomposite (CS-AgNCs)

0.228g of dried Chitosan powder (Plate 2a) was added to 15ml of 1% glacial acetic acid and vigorously stirred for 15 minutes in hot plate with magnetic stirrer at 60^0C to forms homogeneous slurry. The use of glacial acetic acid is to protonate the amine group present in the Chitosan. 0.0456g of Green Synthesized Silver nanoparticles (Plate 1b) was added to the chitosan slurry (in ration 1:4 of AgNP to Chitosan) and continued stirring for about 30 minutes. The mixture (Chitosan and AgNP) turned brown. It was transferred into petri dishes, and dried in a desiccator between 3-5 day at room temperature. It was grinded again into powder (Plate 1c) using mortar and pestle, and sifted to obtain a fine powder using laboratory test sieve (90 micros mesh size, model no- BS410-1-2000, U.K). This reaction is illustrated in equation 3, and plate 1 (a, b and c) in a pictorial form (Govindan *et al* 2012, Olaniyan *et al*, 2016, and Badawy *et al*, 2019).

Simple equation of reaction

$$Chitosan\ (CS) + AgNPs \rightarrow CS\text{-}AgNCs \qquad (3)$$

Pictorial equation showing the physical forms of the reactants (CS and AgNP) and the product (CS-AgNP)

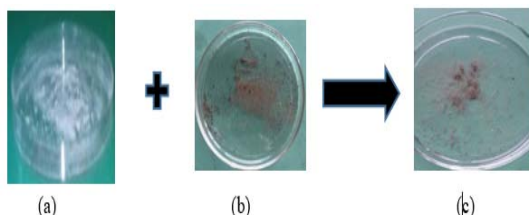(a)   (b)   (c)

Plate 1: (a) Chitosan film (b) Silver nanoparticles (c) Chitosan-Ag nanocomposite powder

2.5. Characterization Techniques

UV-Vis spectrophotometer (BOSCH 750N) was used to determine the optical characteristics of Chitosan slurry, silver nanoparticles, and the polymer composites. The absorption wavelength was determined by placing each aliquot sample taken at time intervals in quartz cuvette operated at a resolution of 1 nm, and deionized water was used as reference solvent.

The morphology and microstructure were determined using Field Emission Scanning Electron Microscope, GEMINI Ultra 55 (FESEM). The samples were fixed on carbon tape and kept for overnight drying. Then the samples were gold coated (100nm) and viewed under the scanning electron microscope operated at 5kV. The Energy Dispersive X-ray analysis was carried out with the EDX Spectrophotometer attached to FESEM GEMINI Ultra 55 to analyze the constituent elements in AgNPs, Chitosan, and Chitosan-Silver nanocomposites (CS-AgNCs).

X-Ray Diffraction was done to determine the crystallinity of the nanoparticles and polymer composites using the Rigaku smartLab diffractometer which has nickel filtered Cu Ka radiation, and operated at 40 kV, 40 mA at room temperature.

The chemical composition of the pure and dried samples of the nanomaterials was analyzed using FTIR Spectrophotometer (Perkin-Elmer 100 series) in the diffuse reflectance mode, from 4000 cm^{-1} – 600 cm^{-1} wavenumbers, at a resolution of 6cm^{-1} in KBr pellet to determine the various functional group that are present in the samples. (Swarnalathan *et al*, 2012).

The data obtained were analyzed using Origin Pro Software

2.6. Antibacterial activities of Chitosan, Silver nanoparticles and Chitosan-Ag Nanocomposites

Antibacterial activity was screened using agar well diffusion method. Mueller Hinton agar plates were swabbed using sterile L-shaped glass rods with mature broth cultures of *A. schubertii, A. hydrophila, V. parahaemolyticus, K. aerogene* and *P. mirabilis.* Plates were then incubated for 24 hours. Using a sterile cork borer, wells of appropriate dimension were made on each Petri dish. 200mg/ml of each of the NPs and polymer composites in sterile DMSO was used, while 200mg/ml of a conventional antibacterial drug (Ofloxacin) was also used as control. 200mg/ml was chosen after other lesser concentrations did not yield positive results. All plates were simultaneously incubated at 37 °C for 24 hrs. After the incubation period, the diameter of inhibition zones of each well was measured. Each sample was tested in two replicate, and the average values were calculated. Minimum inhibitory concentration (MIC) and Minimum bactericidal concentration (MBC) of each of the nanoparticles and the polymer composites were also determined according to CLSI (2012) guide.

2.7. Statistical analysis

Data were subjected to Analysis of variance (ANOVA) using the SPSS (Statistical Package for the Social Sciences) and 10 Microsoft Excel. Means were separated using Duncan multiple range test (DMRT) ($P<0.05$).

3. Result and Discussion

3.1. UV-Visible Spectra of silver nanoparticles, chitosan and chitosan-silver nanocomposites

The results in Figure 4a, 4b and 4c showed the formation of silver nanoparticles, chitosan and CS-Ag NCs. AgNps were first depicted by the Surface Plasmon Resonance (SPR) band (400 nm) at the visible range (Figure 4a). Silver nanoparticles formed at 400nm were found within the standard wavelength range of silver nanoparticle (400-450 nm) according to Ghafouri *et al*, 2017 and Akintayo *et al,* 2020, showing that AgNps were well prepared and thus confirmed their actual formation. In figure 4b, chitosan was found at 240nm, which is typical of a pure chitosan, whose absorption peak usually falls within UV range, 200-300nm (Olaniyan *et al.*, 2016).

Also, Chitosan-Ag nanocomposites were clearly depicted in Figure 4c by a distinct silver nanoparticles' peak at the visible region (400 nm) and chitosan peak at the UV-region (240 nm) on the spectrum which confirmed that the polymer composites was truly formed and composed of silver nanoparticles and Chitosan. This result corroborates the previous finding (Olaniyan *et al*, 2016; Govinda *et al*, 2012; and Zondi *et al*, 2018).
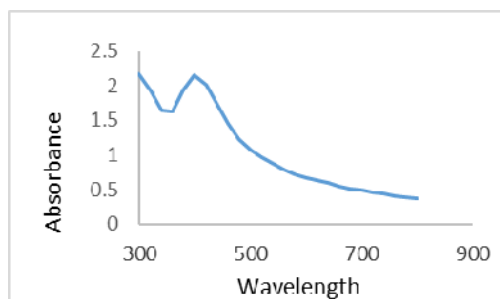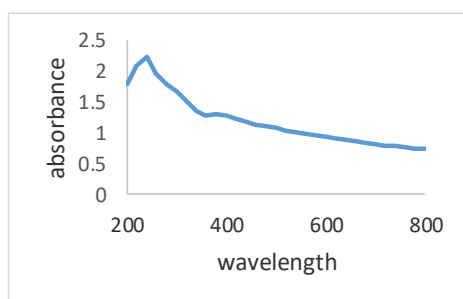

Figure. 4a: UV-Visible specrum of AgNP at 400 nm

Figure 4b. V-Visible Spectrum showing Chitosan at 240nm
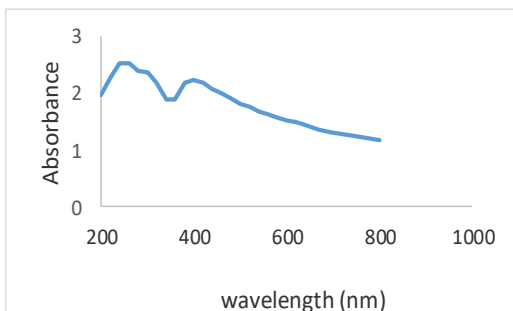
Figure 4c. UV-Visible Spectrum showing Chitosan-silver nanocomposites (CS-AgNCs) at 400nm and 240 nm for AgNP and Chitosan.

3.2. FTIR spectrum of Silver NPs, Chitosan and Chitosan Silver nanocomposites (CS-AgNCs)

The FTIR spectrum shows the bonds which represent functional groups found in AgNPs, CS and CS-AgNC. FTIR absorption peaks were generally found between 4000.00 - 500.00 cm^{-1} range. On silver nanoparticle, the evidence of capping arising by the interaction with the biomolecules present in the plant extract during the reaction are shown by five prominent peaks (Fig 5a) at 3238.89 cm^{-1}, 2924.89 cm^{-1}, 1621.06 cm^{-1}, 1293.76 cm^{-1}, and 1028.65 cm^{-1} which correspond to O-H stretching of

the phenolic compounds, C-H stretching of the fatty acids, C=C stretching of the alkenes, C-O stretching of the 3^0 alcohol group and a C-O-C asymmetric band of ethers respectively. The result depicted the presence of bioactive compounds such as phenols, flavonoids and saponins in the *cassia fistula* leaf extract which participated in AgNPs capping. This result is in tandem with the findings of Mohanta *et al*., 2017 and Danish *et al*., 2022.

The FTIR spectrum of chitosan (Fig. 5b) shows O–H stretching vibration of the phenolic compounds at 3437.63 cm^{-1}, N-H stretching of the amine group at 3258.50 cm^{-1}, C-H stretching of the alkane group (Alkynyl sp3 C-H) at 2921.91 cm^{-1}, O-H bending of the carboxylic acid group at 1659.69cm^{-1}, N-H bending of the amine bond at 1614.70 cm^{-1}, and C-O stretching of the other phenolic compounds at 1375.58 cm^{-1} which matches well with the report by Govinda *et al.*, 2012, Tesfaye *et al.*, 2023 and Zondi *et al.*, 2018.

The FTIR spectrum of CS–Ag nanocomposites was depicted in Fig. 5c. The peaks were found at 3342.15 cm^{-1}, 2916.80 cm^{-1}, 1633.75 cm^{-1}, 1369.36 cm^{-1} and 1027.22 cm^{-1}. These peaks represent functional groups that are found in the polymer composites. The shifting in the CS peaks was also observed in 1750-2000 cm^{-1} range as small irregular bands which may be due to the interaction of Ag with CS in the nanocomposites. These bonds also show that AgNps were bond to chitosan. The absorption peak at 3342.15 cm^{-1} corresponds to O-H stretching of the Phenol group. 2916.80 cm^{-1} correspond to C-H functionality of the alkane group. 1633.75 cm^{-1} corresponds to the C=O stretching of the benzene. 1369.36 cm^{-1} aligns with C-O stretching vibrations of the alcohol group, possibly present in the chitosan matrix while 1027.22 cm^{-1} also align with C-O-C asymmetric band of ethers, which stabilizes the silver nanoparticles in the composites. This result corresponds to the previous finding by Govinda *et al.*, 2012; Gowda and Sriram, 2023.

3.3. XRD pattern of silver nanoparticles, chitosan and Chitosan-Silver Nanocomposites (CS- AgNCs)

The structural properties of the synthesized silver nanoparticles, chitosan and CS–Ag nanocomposites were analyzed using the XRD technique (Fig. 6a, 6b and 6c). This analytical technique is particularly based on diffraction of crystalline material to know the extent of crystallinity. The obtained XRD pattern of silver nanoparticles (Fig. 6a) were observed in the 5 peaks at 2θ angles of 32.37^0, 38.26^0, 44.43^0, 64.08^0, and 77.59^0 which correspond to 101, 111, 200, 220 and 311 reflection planes, respectively. Moreover, the face-centered cubic formation of synthesized AgNPs of various dimensions may be seen in the four intense peaks obtained at 38.26^0 (111), 44.43^0 (200), 64.08^0 (220) and 77.59^0 (311). The peak obtained at 32.37^0 was considered to have been formed due to the crystallization of other organic compounds in the *C. fistula* leaf extract used to synthesize the silver nanoparticles. The results confirmed the crystalline characteristic and face-centered cubic structure of the phytosynthesized AgNPs whose intense bands are in good ascent with reference card (JCPDS Card No. 4-0783) and are in consonance with the reported findings (Bharathi *et al*., 2018; Ahmad, 2023 and Danish *et al.*, 2022).

The obtained XRD pattern for chitosan is shown in Fig 6b. The prominent peaks appeared at 2θ values of 9.40^0,

19.27^0 and 26.28^0 which match well with the literature values (Govinda *et al.*, 2012; Nam and Luong, 2019). They also depicted the crystalline nature of the chitosan. However, the peak at 20.27^0 and other peaks towards the right hand side of the chitosan XRD spectrum are due to chitosan having the cellulose structure which can possess α-type or β-type characteristic peak (Manikadan, 2015). The broadening of 31.80^0, 39.16^0 and 48.19^0 peaks is due to the amorphous nature of the chitosan as a polymorphic biopolymer (Ramon *et al*., 2023). There was no identified impurity peak in the chitosan XRD pattern.

The presence of chitosan and silver peaks as observed from the XRD pattern of CS–Ag nanocomposite is shown in Fig 6c. The graph shows different diffractions at 2θ values of 9.67^0 (020), 20.56^0 (102), 38.34^0 (111), 44.47^0 (200), 64.49^0 (220) and 77.48^0 (311). The prominent CS peaks were observed in the composites graph at 9.67^0 and 20.56^0 while silver nanoparticles were also found at 38.34^0, 44.47^0, 64.49^0 and 77.48^0 on the spectrum showing that both chitosan and silver were involved in the formation of the nanocomposites. These results are similar to the typical Chitosan-silver nanocomposites as described by Selim *et al. (*2020) and Govinda *et al.* (2012).
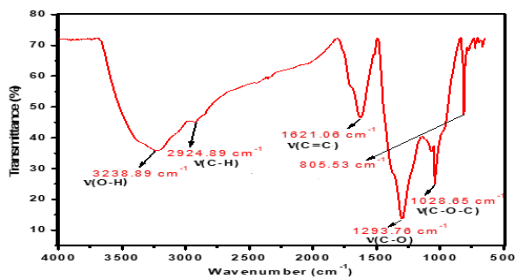

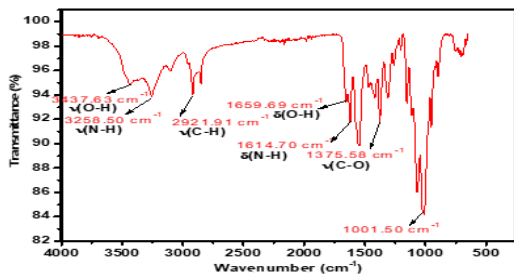Figure 5a: FTIR Spectrum of Silver nanopartccles
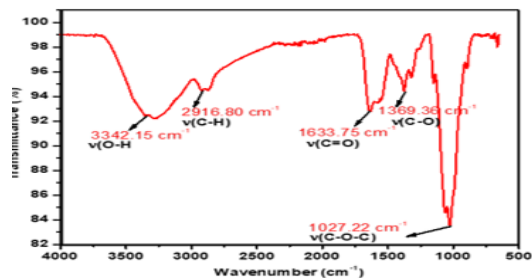

Figure 5b. FTIR Spectrum of chitosan

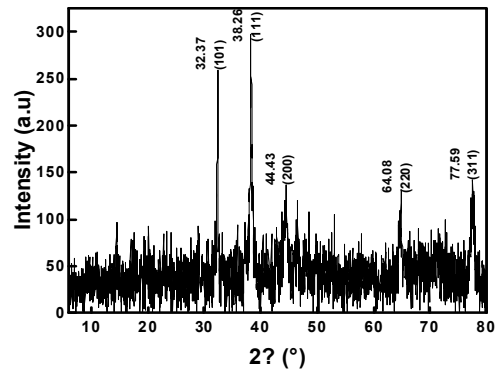**Figure 5c.** FTIR spectrum of CS-AgNCs

Figure 6a. XRD pattern of Silver nanoparticles (AgNPs)

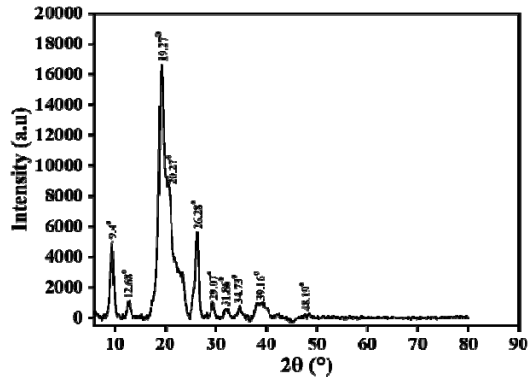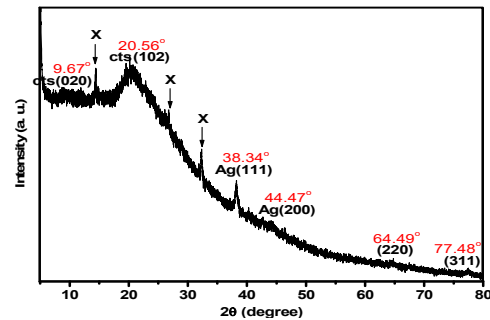**Figure 6b**. XRD pattern of chitosan

Figure 6c: XRD Pattern of CS-AgNCs

3.4 SEM Image of Silver NPs, Chitosan and Chitosan-silver nanocomposites

The scanning electron microscope was used to determine the morphological characteristics of the silver nanoparticles, chitosan and CS-Ag nanocomposites (CS-AgNCs) (Fig. 7a, 7b and 7c). For AgNP, the micrograph depicted individual AgNP in which some are hexagonal and some spherical with average size of 24.94 at x 100, 000 magnifications with some agglomerations (Fig. 7a). The SEM images revealed the bio-molecule coating of the phytosynthesized AgNPs. This layer also confirms the significance of plant extract metabolites in the synthesis and stabilization of AgNPs. These findings are in tandem with those observed by Danish *et al*., (2022), Oves *et al*., (2018) and Banala et al, 2015

SEM analysis of Chitosan nanoparticles depicted cuboidal shape morphology with no agglomeration, and

average size of 30.95 nm at x 100,000 magnification (Fig. 7b).

SEM image of the polymer composite as observed at the surface was shown in figure 7c. It provided the morphology and size of the chitosan-silver nanocomposite which aggregates into irregular structures. The synthesized polymer composites are in the form of aggregates, with low dispersibility but high stability. SEM image also showed that silver nanoparticles were embedded in the chitosan matrix (Govinda *et al.,* 2012) and the composites formed depicted a nose-shaped morphology with irregular size distribution at the average of 62.45nm (Kamari *et al.*, 2009).

3.5 EDX Spectrum of Silver NPs, Chitosan and Chitosan-Ag Nanocomposites

The Energy Dispersive X-ray (EDX) analysis of silver nanoparticles, chitosan and chitosan-Ag Nanocomposites was done to determine the elemental composition of each of the nanoparticles and composites (Figure 8a, 8b and 8c respectively) using EDX analyzer. The typical EDX spectrum of AgNP showed the presence of silver peak in the range of 2.5-4.0 Kev (Fig. 8a). This showed that the synthesized nanoparticles contain silver. The bands also revealed the presence of carboxyl group (C-O) from the plant chemicals used in the synthesis, with carbon and oxygen found between 0.0-0.1kev and 0.1-0.2Kev ranges respectively. However, silver has the highest percentage atomic weight which is responsible for the highest EDX peak, showing that silver nanoparticle is truly formed. This result is in agreement with the previous findings (Banala *et al.*, 2015).

The EDX analysis of chitosan (CON) was depicted in figure 8b. The observed peak was found between 0.0-0.25 Kev, showing that chitosan was purely formed. There were no impurities or any other compound observed in the EDX spectrum.

The typical EDX spectrum of chitosan embedded silver nanocomposites, synthesized at ratio1:5 of AgNP to chitosan is shown in figure 8c. The observed visible peak of Chitosan (CON) at 0.0-0.5Kev and silver (Ag) between 2.5-3.0 Kev depicts the presence of chitosan and silver. Hence, the samples contain chitosan and silver nanoparticles as a polymer composite (Govinda *et al.,* 2012 and Badawy *et al.*, 2019). However, Chitosan showed higher EDX peak above Silver due to its higher percentage composition.

Successful preparation of chitosan silver nanocomposites was also revealed by their physical appearances (Plates 1: a, b and c). Plate 1a shows the maggot-based chitosan powder (whitish colour), plate 1b shows silver nanoparticles. The reaction of the two substances leads to the synthesis of chitosan-silver nanocomposites (Light brown) which indicates a perfect immobilization of silver into chitosan through the reaction as stated in equation 2, yielding a stable chitosan-silver nanocomposite. However, the reaction was conducted in a wet form, in which chitosan used was in form of slurry.
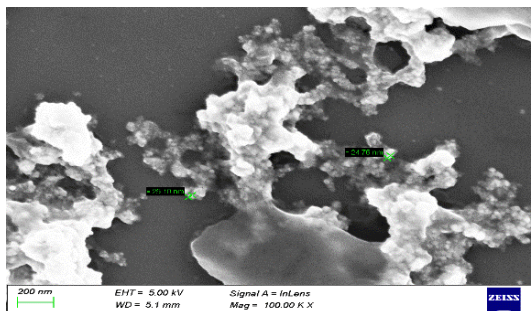

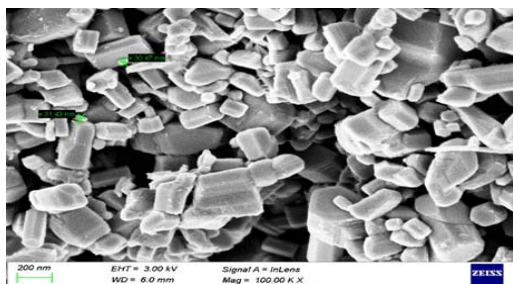**Figure 7a**. SEM image of silver nanoparticles
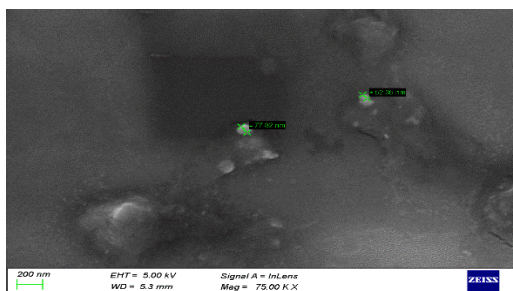

Figure 7b. SEM image of Chitosan

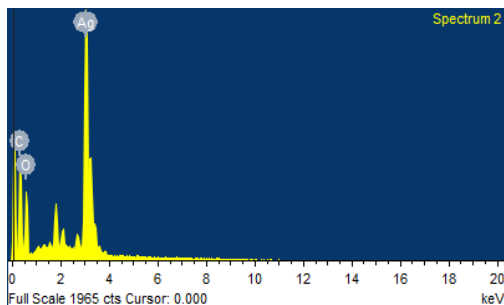**Figure 7c.** SEM Image of Chitosan-Ag Nanocompos

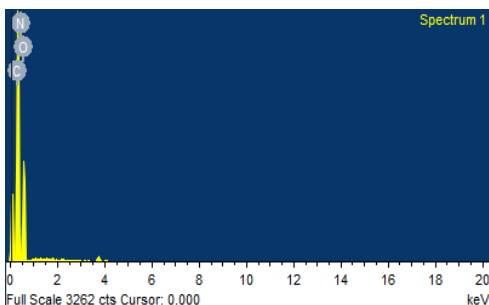**Figure 8a**. EDX Spectrum of Silver nanoparticles (AgNP)

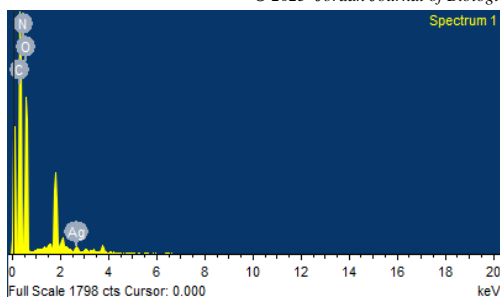**Figure 8b**. EDX Spectrum of chitosan (CS)

Figure 8c. EDX Spectrum of Chitosan-silver nanocomposites (CS-AgNCs)

3.4. in-vitro Antibacterial activity

The results of antibacterial activities of biosynthesized silver nanoparticles (AgNPs), Chitosan (CS) and Chitosan-Silver nanocomposites (CS-AgNCs) using agar well diffusion procedure are shown in Table 1. The result showed zones of inhibition which are measured in millimeters. The values were statistically analyzed using analysis of variance (ANOVA). From the three nanoparticles tested, *A. schubertii* strain depicted the largest inhibition zones with CS-AgNCs (12.50 mm), followed by Chitosan (12.50 mm) and least inhibition zone with AgNP (8.00 mm) along the column.

There was significant difference (P<0.05) in the values of the inhibition zones exhibited by *A. schubertii* in response to the effect of each of the nanoparticles, with the highest sensitivity to CS-AgNCs. *A. hydrophyla* also showed the largest inhibition zone with CS-AgNCs among the three nanoparticles (17.50 mm), followed by chitosan (13.00 mm) and then AgNP (8.50 mm). The difference in the inhibition zones among the nanomaterials was highly significant (P<0.05). A similar trend was found among *V. parahaemolyticus*, *K. aerogene*, and *P. mirabilis* with high sensitivity to CS-AgNCs (16.00 mm, 22.50 mm, and 19.00 mm respectively) than Chitosan (15.50 mm, 15.25 mm, and 19.00 mm respectively) and AgNPs (12.50 mm, 13.00 mm and 13.00 mm respectively). The difference observed in the zone of inhibition by each bacterium on each of the nanoparticle along the column is highly significant (P<0.05) (Table 1). However, antibiotics (Ofloxacin) control displayed higher antibacterial efficacy on each of the bacteria than all the tested nanoparticles (Table 1), except for its limitation due to high toxicity on water and fish, which is a serious concern in aquaculture industry. Moreover, these results showed that CS-AgNCs has an excellent antibacterial potential than Chitosan and AgNPs.

Table 1. Antibacterial sensitivity test of Chitosan-Silver nanocomposites, silver nanoparticles and Chitosan (Mean±SD in Millimeter)

Nanoparticles	*A. schubertii*	*A. hydrophyla*	*V. parahaemolyticus*	*K. aerogene*	*P. mirabilis*
AgNPs	8.00[d]±1.15	8.50[d]±0.58	12.50[c]±0.58	13.00[d]±1.15	13.00[c]±1.15
CS-AgNCs	15.00[b]±2.31	17.50[b]±1.73	16.00[b]±1.15	22.50[b]±0.58	19.00[b]±2.31
Chitosan	12.50[c]±0.58	13.00[c]±1.15	15.50[b]±1.73	15.25[c]±0.87	19.00[b]±1.15
Ofloxacin (Control)	26.50[a]±0.58	26.50[a]±0.58	27.50[a]±0.58	26.50[a]±0.58	26.50[a]±0.58

Concentration- 200mg/ml, AgNPs – Silver Nanoparticles,
Value = Mean±SD
*Superscript of the same alphabet along the column shows that there was no significant difference (P>0.05)
*Superscript of different alphabet along the column shows that there was significant difference (P<0.05)

The ANOVA results of Minimum inhibitory concentration (MIC) is shown in Table 2. The Table depicted the lowest concentration of the nanoparticles at which the pathogens were rendered inactive or prevented from multiplying. According to Table 1, CS-AgNCs depicted the least minimum inhibitory concentration when tested on each of the bacteria isolates (25.04 ± 0.01 mg/mL, 18.50±7.51 mg/mL, 18.75±7.51 mg/mL, 12.03±0.03 mg/mL, and 6.23±0.03 mg/mL) which means that lesser concentration of CS-AgNCs will be needed to inhibit the growth of each of the test bacteria isolates, followed by chitosan (37.50±14.43 mg/mL, 50.01±0.02mg/mL, 18.75±7.22 mg/mL, 12.03±0.03 mg/mL and 37.50±14.43 mg/mL), and AgNP (100.03 ± 0.03 mg/mL, 100.09±0.10 mg/mL, 25.02±0.02 mg/mL, 12.52±0.01 mg/mL, and 25.02±0.02 mg/mL). This shows that higher concentration of AgNP will be needed to inhibit the growth of each of the bacterial isolates than will be needed for CS-AgNCs and Chitosan. There were significant differences (P<0.05) in the MIC recorded on the three nanoparticles against each of the test bacteria islolates (*A schubertii, A. hydrophyla, V. parahaemolyticus, K. aerogene, and P. mirabilis*) along the column (Table 2). This result showed that CS-AgNCs has the highest potential than AgNP and Chitosan against all tested fish pathogens. Nevertheless, Ofloxacin (Control) gives the least concentration that will be needed to inhibit the growth of each of these bacteria (3.13±0.01 mg/mL, 3.13a±0.01 mg/mL 2.13±1.16 mg/mL, 3.13±0.01 mg/mL and 3.13±0.01 mg/mL) but high toxicity of antibiotics on fish and pond water, and constant resistance to antibiotics makes it undesirable in aquaculture industry.

Table 2. Minimum Inhibitory Concentration (MIC) of Chitosan-Silver nanocomposites, Silver nanoparticles and Chitosan (Mean ± SD in mg/mL)

Nanoparticles	*A. schubertii*	*A. hydrophyla*	*V. parahaemolyticus*	*K. aerogene*	*P. mirabilis*
AgNP	100.03[a]±0.03	100.09[a]±0.10	25.02[a]±0.02	12.52[a]±0.01	25.02[b]±0.02
CS-AgNCs	37.50[b]±14.43	18.50[c]±7.51	18.75[b]±7.22	6.25[c]±0.00	37.50[a]±14.43
Chitosan	25.04[c]±0.01	50.01[b]±0.02	12.23[c]±0.03	12.03[b]±0.03	6.23[c]±0.03
Ofloxacin (Control)	3.13[d]±0.01	3.13[d]±0.01	2.13[d]±1.16	3.13[d]±0.01	3.13[d]±0.01

Concentration - 100 mg/ml, Control - Ofloxacin, AgNP – Silver nanocomposites
Value = Mean±SD
*Superscript of the same alphabet along the column shows that there was no significant difference (P>0.05)
*Superscript of different alphabet along the column shows that there was significant difference (P<0.05)

The ANOVA results of Minimum Bactericidal Concentrations (MBC) are shown in Table 3. The Table depicted the lowest concentration of the nanoparticles at which the pathogens were completely destroyed. *A schubertii, A. hydrophyla, V. parahaemolyticus, K. aerogene, and P. mirabilis* strains were completely destroyed when tested with 37.50±14.43 mg/mL, 18.50±7.51 mg/mL, 18.75 ±7.22 mg/mL, 9.38±3.61 mg/mL and 37.50± 14.43 mg/ mL of CS-AgNCs respectively. Also, the minimum bactericidal concentrations when testing the above listed bacterial strain with Chitosan were 50.02±0.02 mg/mL, 50.01 ±0.01 mg/mL, 18.75±7.22 mg/mL, 25.52±0.02 mg/mL and 37.50±14.43 mg/mL respectively. For Silver nanoparticle, the MBC on each of the bacterial isolates were 100.01±0.02 mg/mL, 100.03±0.03 mg/mL, 25.03±0.03 mg/mL, 25.03±0.03 mg/mL and 50.00±0.00 mg/mL respectively. The result depicted a significant difference in the MBC of the nanoparticles on each bacterial strain along the column except on *K. aerogenes* and *P. mirabilis*. *K. aerogene* showed no significant difference in its MBC values when tested on AgNP and Chitosan, but with CS-AgNCs, the difference was highly significant. Likewise, *P. mirabilis* depicted no significant difference in the MBC value when tested on Ofloxacin and CS-AgNC, but with Chitosan and AgNP the difference was highly significant (Table 3).

Table 3. Minimum bactericidal Concentration (MBC) of Chitosan-Silver nanocomposites, silver nanoparticles and Chitosan (Mean ± SD in mg/mL)

Nanoparticles	*A. schubertii*	*A. hydrophyla*	*V. parahaemolyticus*	*K. aerogene*	*P. mirabilis*
AgNP	100.01[a]±0.01	100.03[a]±0.03	25.03[a]±0.03	25.03[a]±0.03	50.00[a]±0.00
CS-AgNCs	37.50[c]±14.43	18.50[c]±7.51	18.75[b]±7.22	9.38[b]±0.00	37.50[b]±14.43
Chitosan	50.02[b]±0.02	50.01[b]±0.01	12.53[c]±0.03	25.52[a]±0.02	6.28[c]±0.03
Ofloxacin (Control)	3.13[d]±0.00	3.13[d]±0.00	3.13[d]±0.00	3.13[c]±0.00	3.13[c]±0.00

Concentration- 100 mg/ml, Control- Ofloxacin, AgNP – Silver nanocomposites
Value = Mean±SD
*Superscript of the same alphabet along the column shows that there was no significant difference (P>0.05)
*Superscript of different alphabet along the column shows that there was significant difference (P<0.05)

Study on antibacterial activities showed that chitosan-silver nanocomposites displayed an excellent antibacterial efficacy against *A. schubertii, A. hydrophila, V. parahaemolyticus, K. aerogene* and *P. mirabilis.* Generally, antibacterial activity of *A. schubertii* among other test pathogens depicted the least sensitivity, although when tested with CS- AgNCs, it was highly sensitive, unlike chitosan and silver nanoparticles. This suggest that while *A. schubertii* can be resistant to varieties of antibiotics, using alternative antibacterial such as CS-AgNCs, chitosan or AgNP can be more effective, including treatment of fish disease caused by *A. schubertii*, and *A. hydrophila,* which are fish pathogens notably responsible for Motile *Aeromonas Septicemia* disease in freshwater fishes, and are capable of causing high motality (Kartikaningsih *et al.*, 2020). Antibacterial sensitivity test depicted higher sensitivity compared to *A. schubertii, and V. parahemolyticus* when tested on CS-AgNCs, although Chitosan was more effective on *V. pahamolyticus* than *A. hydrophila*. This result was supported by Sahar *et al.*, (2018) whose result on biosynthesized AgNP showed that *A. hydrophyla* was very sensitive to AgNP at 37.00±3.08 mm (inhibition zone) and *V. parahaemolyticus* at 10.00±0.77 mm inhibition zones, depicting a high sensitivity. Truong *et al.,* (2020) also reported that chitosan synergized with silver nanoparticles enhance antibacterial effect on pathogenic *A. hydrophyla* causing cytotoxicity and cell disruption leading to bacteria death. Likewise, Salah *et al.,* (2023) reported that chitosan and AgNp exhibited high inhibitory activities against *A. hydrophyla* and subsp. *Hydrophyla* on *A. niloticus* as a novel alternative to antibiotics. The inhibition zones were 15.00 mm and 25 00 mm.

However, *P. mirabilis* and *K. aerogene* showed high sensitivity to CS-AgNCs followed by Chitosan and AgNP. The issue here is that while these pathogens are seen as opportunistic, there is a high tendency for them to behave as obligatory fish pathogen, thus more research is needed on them especially in an *in-vivo* investigation.

Minimum Inhibitory Concentration and Minimum Bactericidal Concentration also showed that all test pathogens were sensitive to the three nanomaterials in the following order: CS-AgNCs > Chitosan > AgNP. According to table 2, at a lower dose (25.04 mg/mL, 18.50 mg/mL, 12.23 mg/mL, 12.03 mg/mL, and 6.23 mg/mL), CS-AgNCs was able to inhibit the growth of each bacterium. The same trend was also observed in the minimum bactericidal concentration (MBC). At 50.02

mg/mL, 50.01 mg/mL, 12.53 mg/mL, 25.52 mg/mL, and 6.28 mg/mL, CS-AgNCs was able to completely destroy each bacterium, showing that CS-AgNP has a surpassing antibacterial efficacy, follow by Chitosan, and Silver nanoparticles (Tables 2 and 3). This result is in tandem with the report by Salah *et al*. (2023) who also conducted a similar research on chitosan and silver nanoparticles. He reported that they both have *in vitro* and *in vivo* antibacterial inhibitory and bactericidal property which made them effective broad spectrum antimicrobial agent against multidrug resistant aquaculture threatening pathogens than antibiotics. He also described the mechanism of their antibacterial action, stating that polymer source nanoparticles (such as chitosan and its composites) absorb and destabilize bacteria cell wall, alter membrane permeability, inhibit DNA replication, translation and transcription, and cause reactive oxygen species generation, while inorganic nanoparticles such as silver nanoparticles penetrate cell walls and release silver ions which interact with protein and enzymes synthesis leading to ribosomal denaturation. Honorary *et al*. (2011) also made it clear that high molecular weight of chitosan on whose matrix silver was embedded to form a composite (CS-AgNCs) is a more effective stabilizer (with its inherent antimicrobial property) owing to its flexibility, and with its synergistic combination with Silver nanoparticles, it greatly increased its antibacterial efficacy. Also the small sizes of the nanoparticles and composites produced aids easy and effective penetration into the bacterial cells. These reports are also supported in other literatures (Truong *et al.,* 2020; Badawy *et al*., 2019; and Tawfik *et al*., 2021).

4. Conclusion

In this study, Chitosan, AgNP and CS-AgNCs were successfully synthesized through eco-friendly techniques which were confirmed by the results obtained from their characterization. The result of antibacterial activity also showed that the nanoparticles and composites (CS-AgNCs, Chitosan and AgNPs) were all effective against the test bacteria pathogens with CS-AgNCs exhibiting the highest antibacterial efficacy.

Consequently, due to their non-toxicity and biocompatibility, these nanomaterials, most especially CS-AgNCs, can serve as effective antimicrobial agents in fish processing, preservation, pond water treatment, inclusion in fish feed for both prophylactic and therapeutic treatments, thereby enhancing fish production in Nigeria and Sub-Sahara Africa, and contribute significantly to sustainable development goals on food security (SDG 2 of the World Health Organization). The use of housefly maggot serves as a mean of converting waste to wealth. It also helps to regulate environmental pollution through low cost and eco-friendly method. The production of chitosan to realize one of the objectives of this research is a potential avenue to reduce poverty and create job opportunity to the teaming population (SGD 1 of the WHO) if employed industrially. Apart from the use of house fly maggots, other examples of arthropods (shrimps, crabs, millipedes), and mollusks could be explored, whose body consists of higher percentage of chitin but are usually treated as wastes and thus disposed. 'These wastes' can be converted to wealth.

Declaration of Interest Statement

The authors declare no conflict of interests on this research article.

References

Abbas G, Jaffery S, Hashmi, AH, Arshad, M, Usmani, SJ, Imran MS, Taweer A, Tariq M, Saleem M, Arshad M, Amin Q, Khan AA, Alvi MA, Shabbir SB, Qureshi RAM, Mustafa A, Iqbal TA, Iqbal A, Hassan M, Abbas S, Zafar R, Abbas W, Abbas H, Mohyyuddin SG, Ismail W, AL-Taey DKA and Shaukat B. 2022. Current prospects of nanotechnology uses in animal production and its future scenario. *Pakistan J of Sci.* 74 (3):203-222. DOI:10.57041/pjs.v74i3.789

Adeshina I, Abdrahman SA and Yusuf AA. 2016. Occurrence of Klebsiella Species in Cultured African Catfish in Oyo State, South-West Nigeria. *Nigeria J of Vet Med*. African Journal on line (AJOL). 37 (1).

Adeyemo OK, Aina OO, Alarape SA, Bodunde O, Hanson L, Wills R, Subasinghe R, Delamare-Deboutteville J, Khor L, Chadag M. 2023. Isolation and characterization of *Klebsiella* and *Pseudomonas* species from farmed African catfish in Nigeria and their implications. *World aqua society*. World conference on Aquaculture, February 23-26, 2023. New Orleans, Louisiana, USA 555 Canal Street New Orleans, LA 70130, United States.

Ahmad A, Mukherjee P and Senapati S. 2003. Extracellular biosynthesis of silver nanoparticles using the fungus *Fusarium oxysporum*. *Colloids & Surfaces B: Biointerf*, 28 (4): 313–318.

Akintayo GO, Lateef A, Azeez MA, Asafa TB, Oladipo IC, Badmus JA, Ojo SA, Elegbede JA, Gueguim-Kana EB, Beukes LS and Yekeen TA. 2020. Synthesis, Bioactivities and cytotoxicity of animal fur-mediated silver nanoparticles. *IOP Conf. series: Mat. Sci. & Eng*. 805:012041. Doi-10.1088/1757-899X/805/1/012041

Akpodiete OJ, Ologhobo AD and Oluyemi JA. 1997. Production and Nutritive Value of Housefly Maggot Meal on Three Substrates of Poultry Faeces. *J. of Appl. Animal Res.*, 12 (1):101-106, DOI: 10.1080/09712119.1997.9706192. https://doi.org/10.1080/09712119.1997.9706192

Akter M, Sikder T, Rahman M, Ullah A, Hossain K, Hosokawa SB, Saito T and Kurasaki M. 2017. A systematic review on silver nanoparticles-induced cytotoxicity: Physicochemical properties and perspectives. *J of Adv Res*. 9:1–16. doi: 10.1016/j.jare.2017.10.008

Badawy MEI, Lotfy TMR and Shawir SMS. 2019. Preparation and antibacterial activity of chitosan-silver nanoparticles for application in preservation of minced meat. *Bulletin of the Nat. Res. Centre*. 43:83 https://doi.org/10.1186/s42269-019-0124-8

Banala RE, Nagati VB, and Karnati PR. 2015. Green synthesis and characterization of Carica papaya leaf extract coated silver nanoparticles through X-ray diffraction, electron microscopy and evaluation of bactericidal properties. *Saudi J. of Bio. Sci*. 22:637-644

Bharathi D, Diviya JM, Vasantharaj S, Bhuvaneshwari V. 2018. Biosynthesis of silver nanoparticles using stem bark extracts of Diospyros Montana and their antioxidant and antibacterial

activities. *J. Nanostructure Chem.* 8:83–92. 10.1007/s40097-018-0256-7

Chen YF, Liang RS, Zhuo XL, Wu XT. 2012. Isolation and characterization of *Aeromonas schubertii* from diseased snakehead, *Channa maculata* (Lacepède). *J of Fish Diseases* 35(6):421-30. DOI:10.1111/j.1365-2761.2012.01362.x

CLSI. 2014. Clinical and Laboratory Standards Institute. **Performance Standard for Antimicrobial Susceptibility Testing**; Twenty-fourth information supplement. CLSI Document M100-S24, Wayne, 34(1).

Cristiano C, Dolores VP, Maria RG, Siyuan D, Roberta C, and Piera Di Martino. 2019. Chitin and Chitosans: Characteristics, Eco-Friendly Processes, and Applications in Cosmetic Science- a review. *Marine Drug*. Vol. 17:(1) 369:1-30. doi:10.3390/md17060369

Danish M, Shahid M, Ahamad L, Raees K, Hatamleh AA, Al-Dosary MA, Mohamed A, Abdulrhman Y, Wasel A, Singh UB and Danish S. 2022. Nano-pesticidal potential of Cassia fistula (L.) leaf synthesized silver nanoparticles (Ag-CfL-NPs): Deciphering the phytopathogenic inhibition and growth augmentation in Solanum lycopersicum (L). *Frontiers in Mic.* 10:1-18

Dayem, A.A; Hossain, M.K.; Lee, S.B.; Kim, K.; Saha, S.K.; Yang, G.-M.; Choi, H.Y.; Cho, S.-G. 2017. The Role of Reactive Oxygen Species (ROS) in the Biological Activities of Metallic Nanoparticles. *Int. J. Mol. Sci*, 18, 120.

Fajardo C, Martinez-Rodriguez G, Blasco J, Mancera JM, Thomas B, De Donato M. 2022. Nanotechnology in aquaculture: Applications, perspectives and regulatory challenges. *Aqua and Fish*. Vol. 7(2):188-200. https//doi.org/10.1016/j.aaf.2021.12.006.

Ghafouri SM, Entezari M, Taghva A and Zahra Tayebi, Z. 2017. Biosynthesis and evaluation of the characteristics of silver nanoparticles using *Cassia fistula* fruit aqueous extract and its antibacterial activity. *Adv. Nat. Sci*.: Nanosci. Nanotechnol. https://doi.org/10.1088/043-6254/aa92bb

Govindan S, Nivethaa EA, Saravanan R, Narayanan V, Stephen A. 2012. Synthesis and characterization of chitosan–silver nanocomposite. *J. Appl Nanosci*. 2:299–303. springerlink.coms

Gowda PS and Sriram S. 2023. Green synthesis of chitosan silver nanocomposites and their antifungal activity against *Colletotrichum truncatum* causing anthracnose in chillies. *Plant nanobio*. Vol. 5. doi. https/doi.org/10.101016/j.plana.

Hezron L, Madalla N and Sebastian W, Chenyambuga SW. 2019. Mass production of maggots for fish feed using naturally occurring adult houseflies (*Musca domestica*). *Livestock Res for Rural Dev*. 31(4)

Honary S, Ghajar K, Khazaeli P and Shalchian P. 2011. Preparation, Characterization and Antibacterial Properties of Silver-Chitosan Nanocomposites Using Different Molecular Weight Grades of Chitosan. *Tropical J of Pharm Res*. 2011. 10 (1): 69-74.

Huang S, Wang L, Liu L, Hou Y, and Lu-Li L. 2015. Nanotechnology in agriculture, livestock, and aquaculture in China. A review. *Agron. Sustain. Dev.* 35:369–400. DOI 10.1007/s13593-014-0274-x

Irshad MD, Zafaryab MD, Man S, and Moshahid M. 2014. Comparative Analysis of the Antioxidant Activity of *Cassia fistula* Extracts, *Int J of Med Chem* Vol.12.

Islam NU, Jalil K and Shahid M. 2021. Green synthesis and biological activities of gold Nanoparticles functionalized with *Salix alba*. *Arab J Chem*. http://doi.org/10.1016/j.arabj

c.2015.06.025

Kamari A, Ngah WS, Chang MY and Cheah ML. 2009. Sorption of acid dyes unto GLA and H_2 SO_4 cross-linked Chitosan beads. *Desalination*. 249:1180-1189

Kartikaningsih H, Yahya F, Rohman Z and Jaziri AA. 2020. Characteristics of *Aeromonas hydrophila*-infected Catfish (*Clarias sp.*). International Conference on Sustainable Aquatic Resources IOP Conf. Series: Earth and Environmental Science. 10:493-500. 012036 *IOP Pub*. doi:10.1088/1755-1315/493/1/012036

Kaur P, Choudhary, A and Thakur RR. 2012. Synthesis of Chitosan-Silver Nanocomposites and their Antibacterial Activity. *Int. J. of Sci and Eng. Res*, Volume 4, Issue 4, ISSN 2229-5518

Kim MW, Han YS, Jo H. 2016. Extraction of chitin and chitosan from housefly, *Musca Domestica,* pupa shells. *Entomol Res*. 46: 324–328.

Manikandan A and Sathiyabama M. 2016. Preparation of Chitosan nanoparticles and its effect on detached rice leaves infected with Pyricularia grisea *Int. J. of Bio. Macro*. 84:58-61. doi: 10.1016/j.ijbiomac.2015.11.083.

Mohanta YK, Panda SK, Jayabalan R, Nanaocha SN, Bastia AK and Mohanta TK. 2017. Antimicrobial, Antioxidant and Cytotoxic Activity of Silver Nanoparticles Synthesized by Leaf Extract of *Erythrina suberosa* (Roxb.). *Frontier in molecular biosci*. 4 (14):1-7. doi: 10.3389/fmolb.2017.00014

Nam NH and Luong NH. 2019. Nanoparticles: synthesis and applications. Materials for biomedical applications. doi: 10.1016/B978-0-08-102814-8.00008-1. 211-240.

Nikalje AP. 2015. Nanotechnology and its Applications in Medicine. *Medicinal chem*. 5 (2): 81-89. http://dx.doi.org/10/4172/2161-0444.1000247.

Nowack B, Krug HF and Height M. 2011. 120 years of Nanosilver History, Implication for Policy Makers. *Environ. Sci. Technol.*, 45: 1177–1183.

Olaniyan OJ, Dare EO, Adetunji OR, Adedeji OO and Ogungbesan, SO. 2016. Synthesis and Characterization of Chitosan-Silver Nanocomposite Film Nano Hybrids and Composites ISSN: 2297-3400, 11:22-29. Doi:10.4028/www.scientific.net/NHC. *Trans Tech Pub*, Switzerland

Olugbojo JA and Ayoola SO. 2015. Comparative studies of bacteria load in fish species of Commercial importance at the aquaculture unit and lagoon front of the University of Lagos, Lagos. *Int J of Fish and Aqua*. 7(4):37-46. www.academicjournals.org/ijfa

Oves M, Rauf MA, Aslam M, Qari HA, Sonbol H, Ahmad I, ZamanGS, and Saeed M. 2021. Green synthesis of silver nanoparticles by *Conocarpus Lancifolius* plant extract and their antimicrobial and anticancer activities. *Saudi J of Bio Sci* 29(1): 460–471. doi: 10.1016/j.sjbs.2021.09.007

Ramon DR, Torres SP, Tenorio AY, Gómez SA, and Valencia AA. 2023. Chitosan: Properties and Its Application in Agriculture in Context of Molecular Weight *Polymers*. *15*(13), 2867; https://doi.org/10.3390/polym15132867

Sahar WM., and Hala H. Abd El-latif. 2018. Characterization and application of biosynthesized AgNP by marine pseudomonas. *J. of Pure and Appl. Micro.* 12 (3):1289-1299. https://doi.org/10.22207/JPAM.12.3.31.

Salah MA, Eissa AE, Abdel-Razek, N and El-Ramlawy, AO. 2023. Chitosan nanoparticles and green synthesized silver nanoparticles as novel alternatives to antibiotics for preventing *A. hydrophila subsp.*

hydrophila infection in Nile tilapia, *Oreochromis niloticus. Int J of Vet Sci & Med..* 11(1): 38–54. Published online doi: 10.1080/23144599.2023.2205338

Selim YA, Maha A. Azb MA, Islam Ragab I and Abd El-Azim MHM. 2020. Green Synthesis of Zinc Oxide Nanoparticles Using Aqueous Extract of *Deverra tortuosa* and their Cytotoxic Activities. *Sci Reports*. 10:3445 |https://doi.org/10.1038/s41598-020-60541-1 4

Song YS, Seo DJ, Ju WT, Park RD and Jung WJ. 2014. Preparation of chitosan with sodium hydroxide according to condition of temperatures. *J of Chitin and Chitosan* 19: 8–14.

Swarnalathan R, Christina RS and Payas B. 2012. Evaluation of in vitro antidiabetic activity of *Sphaeranthus amaranthoides* silver nanoparticles. *Int J of Nanomat Biostructure*, 2 (3): 25–29.

Tawfik M, Tawfik I, Ahmed MA. El-Masry. 2021. Preparation of Chitosan Nanoparticles and its Utilization as Novel Powerful Enhancer for Both Dyeing Properties and Antimicrobial Activity of Cotton Fabrics. *Biointerface Res in Appl Chem*. 11 (5):13652 – 13666. https://doi.org/10.33263/BRIAC115.1365213666

Tesfaye, M., Gonfa, Y., Tadesse, G., Temesgen,T and Periyasamy, S. 2023. Green synthesis of silver nanoparticles using *Vernonia amygdalina* plant extract and its antimicrobial activities. *Heliyon*. 9(6):11-20. doi: 10.1016/j.heliyon.2023.e17356

Thai HHP, Kim D, Thi C, Quach Van Q. Nguyen, PT Nguyen, TL. 2023. Prevalence and antibiotic resistance of Aeromonas schubertii causing internal white spot disease on snakehead fish, Channa striata, in the Mekong Delta, Vietnam. *J of World Aqua Soc*. 23: 1-17. DOI: 10.1111/jwas.12954

Truong T, Nguyenb D, Hien Quoc Nguyena. 2020. Nanocomposite of silver nanoparticles/diatomite against bacteria pathogens of catfish. *Int J of Vet sci & med*. Hanh Thi Research and Development Center for Radiation Technology, Vietnam Atomic Energy Institute, 202A, Street 11, Linh Xuan Ward, Thu Duc District, Ho Chi Minh City.

Younes I and Rinaudo M. 2015: Review Chitin and Chitosan Preparation from Marine Sources. Structure, Properties and Applications. *Marine drugs*. 13: 1133-1174; doi: 10.3390/md13031133.ISSN:1660-3397 www.mdpi.com/journal/marinedrugs

Zhai W, Wang WQ, Zhu X Jia, X, Chen, L. 2023. Pathogenic infection and microbial composition of yellow catfish (*Pelteobagrus fulvidraco*) challenged by *Aeromonas veronii* and *Proteus mirabilis. Aqua and Fish. 8(2): 166-173*

Zondi N, Moloto MJ, Mubiayi1 PK, Sibiya PN. 2018. Green synthesis of chitosan capped Silver nanoparticles and their antimicrobial activity. *MRS. Adv. Mat. Res. Soc.* DOI: 10.1557/adv.2018.368

Zhuling R, Yan C, Shifeng W, Shubin L., Youfei X, Jiaqing T, Yun S. Weiliang, G,a Yongcan, Z. 2019. First case of Aeromonas schubertii infection in brackish water wild Nile tilapia, *Oreochromis niloticus*, in China. *Aquaculture*. 10.1016/j.aquaculture.2018.11.036.